RSC Advances

PAPER

View Article Online
View Journal | View Issue

Cite this: *RSC Adv.*, 2024, **14**, 2402

Synthesis of ZnO and PEG-ZnO nanoparticles (NPs) with controlled size for biological evaluation

Mahnoor Khan,[a] Bashir Ahmad,[a] Khizar Hayat,[b] Fahad Ullah,[c] Nourreddine Sfina,[d] Muawya Elhadi,[e] Abid Ali Khan,[*af] Mudasser Husain[g] and Nasir Rahman[h]

Received 1st November 2023
Accepted 3rd January 2024

DOI: 10.1039/d3ra07441b

rsc.li/rsc-advances

The objective of this research was to produce the smallest possible ZnO nanoparticles through an adapted wet chemical process and subsequently, to fabricate a core–shell structure utilizing polyethylene glycol (PEG) as the shell component. The synthesis, size, and shape of the NPs were confirmed using advanced techniques. The resulting clustered NPs were round and had a size of 9.8 nm. Both plain and core–shell NPs were tested for their antibacterial properties against multi-drug resistant bacteria strains (*E. cloacae*, *E. amnigenus*, *S. flexneri*, *S. odorifacae*, *Citrobacter*, and *E. coli*), with concentrations of 500, 1000, and 1500 μg ml^{-1} used for testing. Both types of NPs demonstrated antibacterial activity against the tested pathogens, with the core–shell NPs being more effective. The synthesized NPs were biocompatible with human red blood cells, with a low level of hemolysis observed. The biocompatibility of the core–shell NPs was significantly enhanced by the presence of the PEG added as the shell. In addition, their effectiveness as photosensitizers for cancer treatment *via* photodynamic therapy (PDT) was evaluated. MTT assay was used to evaluate the cytotoxicity of ZnO and PEG-ZnO, and the results showed that these NPs were able to generate ROS inside tumor cells upon irradiation, leading to apoptosis and cell death, making them a promising candidate for PDT.

Introduction

Nanotechnology is an emerging field of science and development and this field is creating endless possibilities for betterment of human life. However, the misuse of antibiotics and other different drugs, is a major cause of increasing bacterial resistance to these molecules. Scientists are struggling to find new and innovative methods for combating the bacterial resistance to antibiotic drugs and are trying to find new and alternative methods to fight against deadly diseases for better quality of human life. Nanotechnology might have the solution to all the problems, because of its broader horizon.

As per the reported literature, ZnO NPs has a wide range of biological applications and is also biocompatible as compared to other metal oxide NPs.[1] ZnO NPs being the most commonly utilized nanomaterial in commercial products, their toxicity and efficiency is regularly monitored, however, few researchers have reported slight toxicity when used in higher concentrations. Therefore, for reducing its toxicity different biocompatible and biodegradable materials are used. Some of the commonly used materials are polyethylene glycol (PEG),[2] albumin, polyethylene oxide, dextran and aspartic acid.[3]

In the current study, we used PEG because PEG coating increases the stability of NPs in biological systems, it also helps in tissue distribution as well as aid in their entry into the cells. They also increase the retention time of NPs inside biological cells and decreasing toxicity, thus making NPs more biocompatible.[4,5] The objectives of the current study were to synthesize ZnO NPs *via* chemical route followed by PEGylation processes and finally to figure out its biological applications.

Synthesis of ZnO nanoparticles

Wet chemical route was used to synthesize zinc oxide nanoparticles (ZnO NPs). This technique can be used to synthesize a sufficient quantity and control morphology of the desired material. Furthermore, it is a single step synthesis technique in which no surfactant was used to control the morphology of ZnO NPs. The schematic in Fig. 1 shows the synthesis of ZnO nanoparticles *via* wet chemical route. Initially, an amount of 4.18 g of zinc acetate dihydrate was weighted using sensitive digital balance. It was then dissolved in methanol of 220 ml

[a]*Centre of Biotechnology and Microbiology, University of Peshawar, KP 25120, Pakistan*
[b]*Department of Physics, Abdul Wali Khan University, Mardan, KP 23200, Pakistan*
[c]*Northwest School of Medicine Peshawar, KP 25120, Pakistan*
[d]*Department of Physics, College of Sciences and Arts in Mahayel Asir, King Khalid University, Abha, Saudi Arabia. E-mail: nsfina@kku.edu.sa*
[e]*Department of Physics, Faculty of Science and Humanities, Shaqra University, Ad-Dawadimi 11911, P. O. Box 1040, Saudi Arabia. E-mail: muawya2005@gmail.com*
[f]*Department of Chemical Sciences, University of Lakki Marwat, KP 28420, Pakistan*
[g]*State Key Laboratory for Mesoscopic Physics and Department of Physics, Peking University, Beijing 100871, P. R. China. E-mail: 2201110247@stu.pku.edu.cn*
[h]*Department of Physics, University of Lakki Marwat, Lakki Marwat, 28420, KPK, Pakistan. E-mail: nasir@ulm.edu.pk*

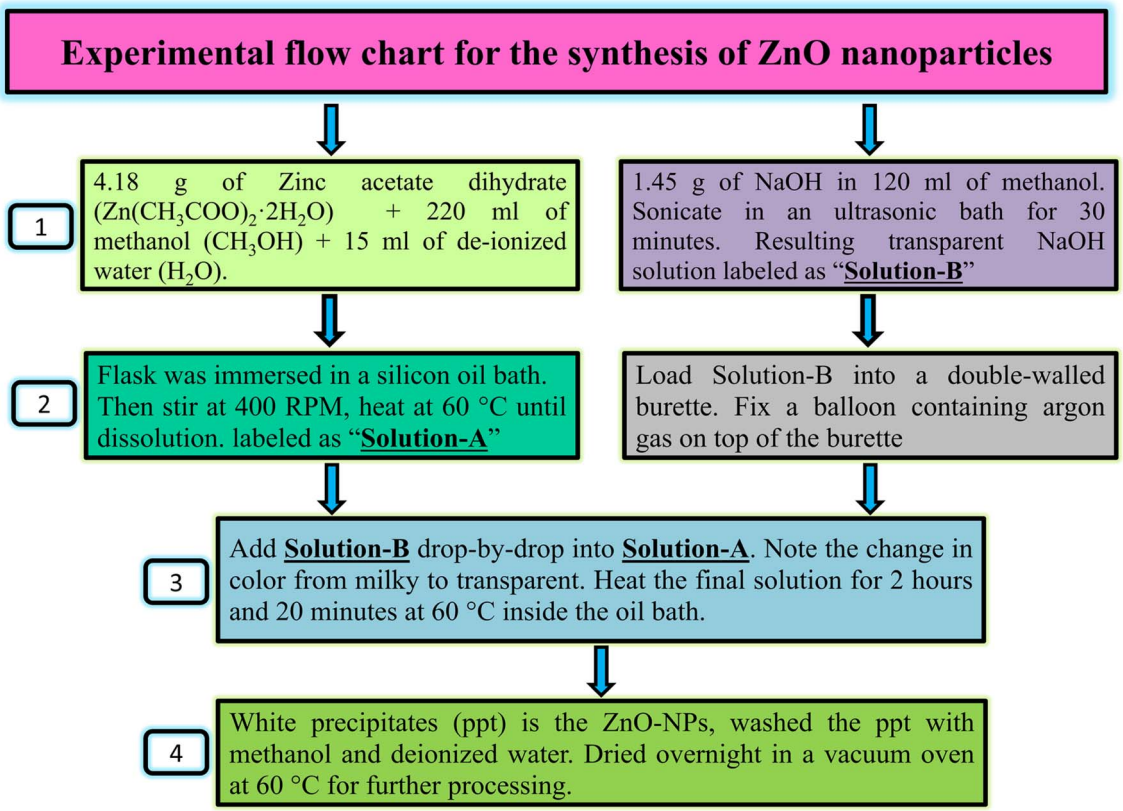

Fig. 1 Schematic presentation of ZnO NPs synthesis *via* chemical route.

taken in a round bottom flask of capacity of 500 ml. De-ionized water of 15 ml was also added to this solution. The flask was then immersed in a silicon oil bath. The solution was stirrer at 400 RPM inside oil bath under constant heating at 60 °C until $Zn(CH_3COO)_2 \cdot 2H_2O$ completely dissolved in methanol. This solution is labeled as "Solution-A" as shown in Fig. 1. Likewise, another solution of sodium hydroxide (NaOH) was prepared in a separate flask. NaOH of 1.45 g was dissolved in 120 ml of methanol followed by its sonication in ultrasonic bath for around 30 minutes. The final NaOH transparent solution obtained is named as "Solution-B" as shown in Fig. 1. Solution-B was then loaded into a double walled burette already fixed on round bottom flask. A balloon containing argon gas was fixed on top of burette to accomplish the reaction process in a controlled inner atmosphere. NaOH solution was subsequently added drop-by-drop into the zinc acetate solution. It was noted that the color of reaction mixture was first become milky just after the addition of few drops of NaOH solution and then it turned to a transparent like solution after further addition of NaOH solution. The final solution was further heat treated for 2 hours and 20 minutes at 60 °C inside the oil bath. During this time white precipitates of ZnO nanoparticles were obtained. These precipitates were thoroughly washed several times with methanol and deionized water to remove any impurities, residuals or any other unbound molecules to get pure ZnO NPs.[6] Finally, it was dried for overnight in a vacuum oven at 60 °C.

PEGylation of ZnO NPs

Fig. 2 shows the process of PEGylation of zinc oxide nanoparticles. For PEGylation, prepared ZnO NPs were mixed with distilled water (named as Solution A). In another flask, PEG (4000 MW) was dissolved in distilled water separately (named as Solution B). These two solutions were then mixed and the final mixture was kept on a magnetic stirrer for 48 hours at room temperature at a medium speed. The solution were then transferred to oven and kept overnight for dryness at 60 °C to get PEG coated ZnO NPs.[7]

Characterization of ZnO NPs

The crystal structure of ZnO NPs was examined using X-ray diffractometer (XRD). Cupper CuKα1 radiations at 25 °C (wavelength $\lambda = 1.5406$ Å) was used as X-ray source. The particle size of zinc oxide nanoparticles was investigated using a Transmission Electron Microscope (TEM) with the following specifications: Model JEM-2100 by JEOL, Japan. The optical band gap of PEGylated and non-PEGylated ZnO NPs was analyzed using UV/VIS spectrometer in the wavelength range of 200 to 900 nm. Fourier transforms infra-red (FTIR) spectroscopy was carried out to study the formation of core bonds of Zn with O *i.e.*, the functional groups of synthesized ZnO NPs.[8]

Antibacterial activity of ZnO NPs

Well diffusion method was performed to check the antibacterial efficacy of our prepared NPs against 6 MDR bacteria

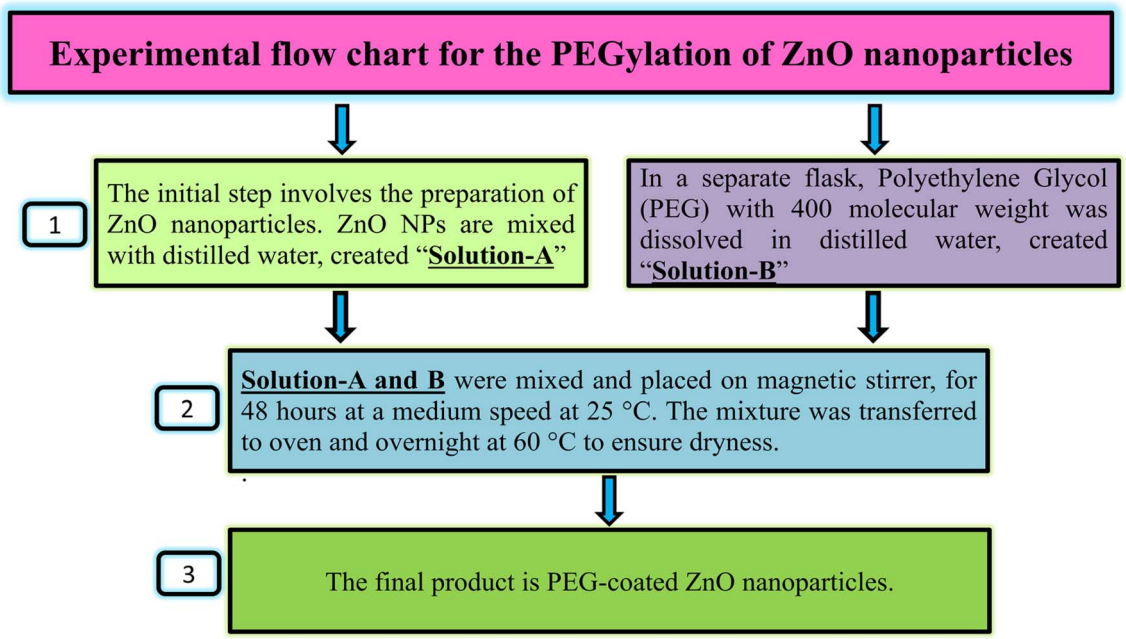

Fig. 2 Schematic presentation of PEG-ZnO nanoparticles synthesis.

(*Citrobacter*, *Shigella*, *Serratia odorifacae*, *Enterobacter cloacae*, *Escherichia coli* and *Enterobacter amnigenus*). Broth cultures of bacterial strains were evenly spread on MacConkey Agar. Sample solution of our nanoparticles was poured in wells and the plates were then placed in sunlight for a few minutes to activate the NPs. Zone of inhibition was recorded the next day for each strain.[9]

Hemolysis assay of ZnO NPs

Two milliliters (2 ml) of fresh blood were collected from volunteers and then mixed with phosphate-buffered saline (PBS) solution. Eppendorf tubes containing the diluted blood were subsequently treated with various concentrations of NP solutions (30, 50, 70, and 1000 μg ml^{-1}). As a positive control, Triton X-100 was employed. All tubes were incubated for 3 hours at 37 °C, followed by centrifugation at 1500 rpm for 15 minutes. The resulting supernatant was collected, and its absorbance was measured at 576 nm using the following formula.[10,11]

$$\text{Hemolysis } (\%) = \frac{\text{OD of sample} - \text{OD negative control at 540 nm}}{\text{OD of positive control} - \text{OD negative control at 540 nm}} \times 100$$

Brine-shrimps cytotoxicity assay of ZnO NPs

Sea salt was dissolved in double distilled water to make artificial hatching media for brine shrimps. Brine shrimps were grown in the prepared media for 48 hours. Then thirty (30) live larvae were transferred from the media to six (6) Petri dishes each. In individual Petri dishes, NPs solutions at varying concentrations (10, 100, and 1000 μg ml^{-1}) were added, followed by a 24 hour incubation at 25 °C under suitable aeration and controlled lighting conditions.[12]

$$\text{Mortality } (\%) = 100 - \frac{\text{shrimps in sample}}{\text{total shrimps}} \times 100$$

Photodynamic therapy (anticancer activity)

During photodynamic therapy, 200 μl of growth media were used to seeding hep2c culture cell lines in two 96-well plates and the cells were grown overnight to proliferate. Various concentrations of ZnO and PEG-ZnO NPs were used in the cell incubation experiments. To assess the effects of UV irradiation on the cytotoxicity of ZnO NPs and PEG-ZnO NPs, one of the two plates was exposed to UV radiation for two minutes using a UV transilluminator. All of the cells underwent a further 48 hours of incubation. Later, the cytotoxicity and cell viability of ZnO NPs were assessed using the MTT assay.[13]

Results and discussion

Analysis of X-ray diffraction (XRD)

Fig. 3 displays the X-ray diffraction pattern of ZnO-NPs. The red color pattern shows the zinc oxide standard XRD data. All peaks in the XRD pattern were indexed using JCPDS card #: 36-1451. It is obvious from the figure that all peaks in the XRD pattern of ZnO NPs matched well with the standard ZnO X-rays powder diffraction data. No extra peak was observed this indicates the formation of single phase polycrystalline zinc oxide nanoparticles. ZRD peak's broadening suggests that the constituents of ZnO powder are smaller in size and in the nano regime. In order to calculate the average primary crystallite size or grain size of ZnO-NPs, the following Scherrer equation was used.

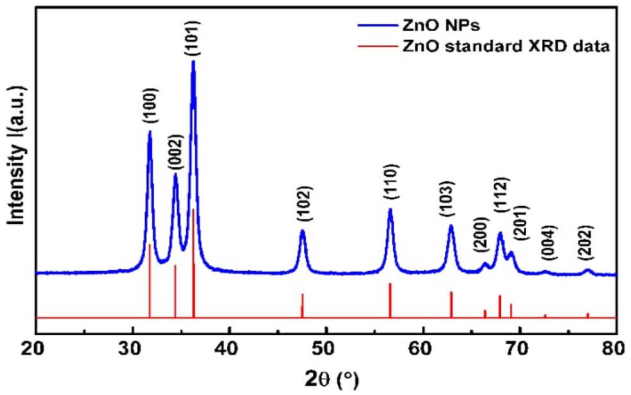

Fig. 3 XRD pattern of ZnO NPs synthesized *via* chemical method. The red color graph shows the standard ZnO XRD pattern.

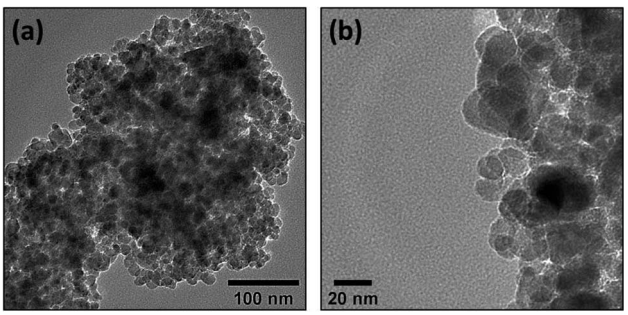

Fig. 4 Transmission electron microscope images of zinc oxide nanoparticles recorded at (a) low & (b) high magnifications.

$$D = \frac{K\lambda}{\beta \cos \theta} \quad (1)$$

Here, D, K, λ, β, and θ represent the crystallite size, the Scherrer constant (assumed as 0.9 for particles with a spherical geometry), the wavelength of the X-ray source (0.15406 nm), the full width at half maximum (FWHM), and the peak position in radians, respectively. Origin software was used to determine the FWHM and peaks position of all crystalline peaks. Using eqn (1), an average primary crystallite size of 9.80 nm was obtained.

Analysis of transmission electron microscopy (TEM)

Transmission electron microscopy (TEM) was utilized to determine the size and morphology of ZnO NPs. In Fig. 4(a) and (b), low and high magnification TEM images of ZnO nanoparticles are presented, respectively. The low magnification TEM image reveals that ZnO nanoparticles exhibit a spherical shape, and all particles appear to be nearly uniform in size. Fig. 4(b) clearly indicates an average particle size of approximately 10 nm, consistent with the findings obtained from XRD analysis.

Analysis of FTIR

Fourier transform infrared spectroscopy (FTIR) was performed to ascertain the presence of functional groups in both ZnO and

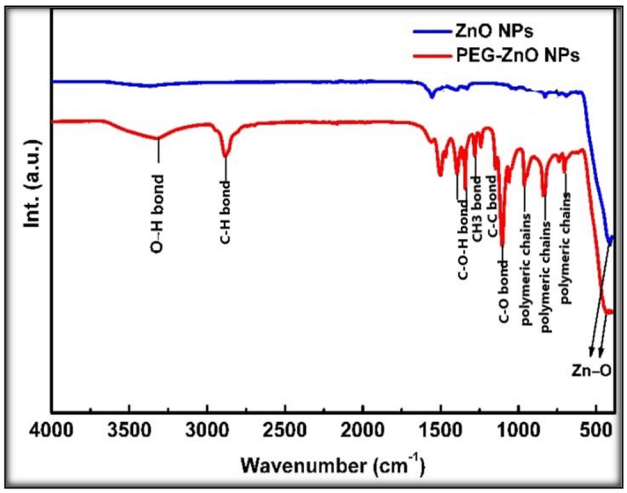

Fig. 5 FTIR spectra of PEGylated and non-PEGylated ZnO-NPs.

PEGylated ZnO NPs, as shown in Fig. 5. ZnO's synthesis was confirmed by its peak at 526 cm^{-1}, On the other hand, the presence of a peak at 535 cm^{-1} verified the absorption band characteristic of ZnO metal oxide. The peak in the range between 3200 and 3500 cm^{-1} region of the PEG-ZnO is caused by the absorption of O–H group stretching vibration. The peaks between 675 and 850 cm^{-1} are assumed to be caused by long polymeric chain bending.

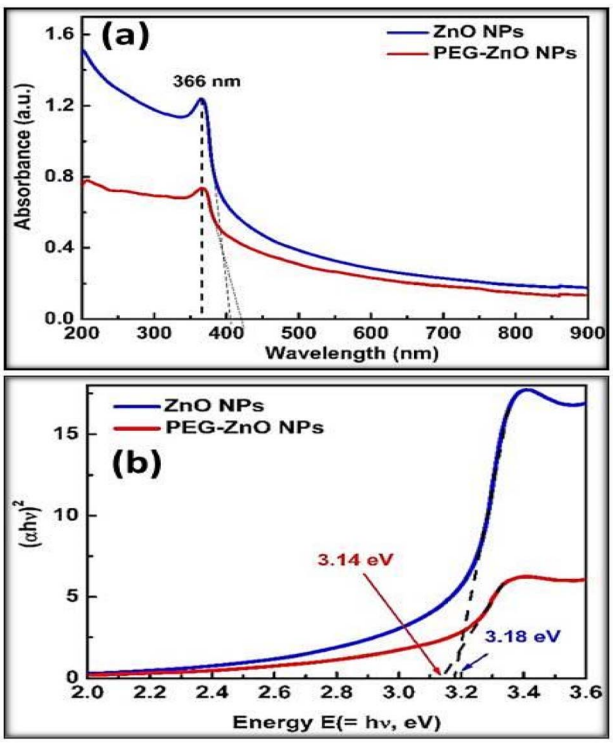

Fig. 6 (a) Absorbance spectrum and (b) energy band gap calculation (using Tauc plot) of PEGylated and non-PEGylated ZnO-NPs.

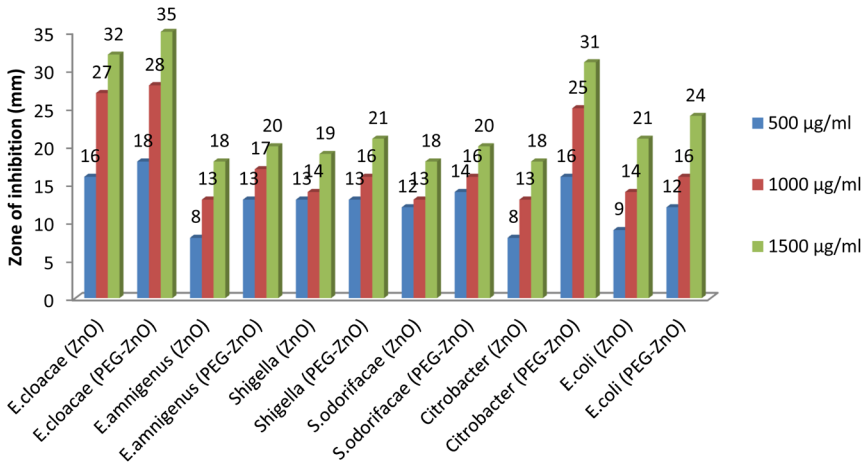

Fig. 7 Antibacterial activities of the plain and PEG-ZnO.

Analysis of UV/VIS absorption spectroscopy

The absorption spectra of PEGylated and non-PEGylated ZnO-NPs were shown in Fig. 6(a). Both spectra have shown the maximum absorbance in the UV-visible region at wavelength of 366 nm. However, ZnO-NPs have more absorption as compared to PEGylated ZnO-NPs. This reduction in the absorption of UV-visible photons by PEGylated-ZnO NPs is the confirmation of the successful attachment of polyethylene glycol (PEG) molecules at surface around ZnO-NPs. As the presence of PEG polymers on the surface of ZnO can reduce the absorption intensity of ZnO NPs, it results in a slight red shift in wavelength absorption.

Fig. 6(a) illustrates the UV-vis absorption spectra of both PEGylated and non-PEGylated ZnO particles. ZnO NPs display a broad absorption peak at 366 nm, corresponding to a band gap energy of 3.18 eV. In contrast, the absorption of PEG-ZnO NPs also centers around 366 nm, with a band gap energy of 3.14 eV.

Antibacterial activity

Antibacterial activity was conducted to see if the synthesized NPs are capable of inhibiting the virulence microorganisms. Agar well diffusion method was used with different dose concentration (500, 1000 and 1500 µg ml^{-1}) of the synthesized NPs. Antibacterial activities were recorded in terms of zone of inhibition. Both the Plan and PEG-ZnO NPs were effective against the targeted microorganisms, however, both were more effective against *E. cloacae* as shown in the Fig. 7.

Hemolysis

Both of the samples (plain and PEG-ZnO) were non-toxic at concentrations of 30, 50 and 70 µg ml^{-1} with a hemolysis % of 1.8, 2 and 4 for plain ZnO NPs and 0.79, 1.1 and 1.5 for PEG-ZnO NPs (Fig. 8).

Brine shrimp cytotoxicity assay

The mortality % was 7, 17 and 34 respectively for 10, 100 and 1000 µg ml^{-1} of plain ZnO NPs and 0, 7 and 20 for 10, 100 and 1000 µg ml^{-1} of PEG-ZnO NPs (Fig. 9).

Photodynamic therapy (anticancer activity)

The findings demonstrated a clear, dose-dependent correlation between the concentration of pure ZnO NPs and cellular viability. However, concentrations exceeding 60 µg ml^{-1} exhibited considerable toxicity, leading to a significant decrease in cellular viability. In contrast, the results for UV-irradiated

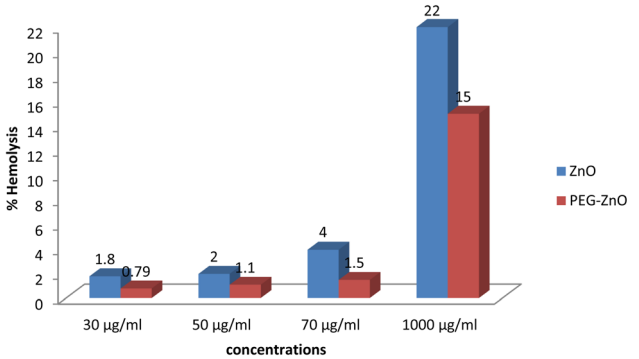

Fig. 8 Hemolytic activities of the plain and PEG-ZnO.

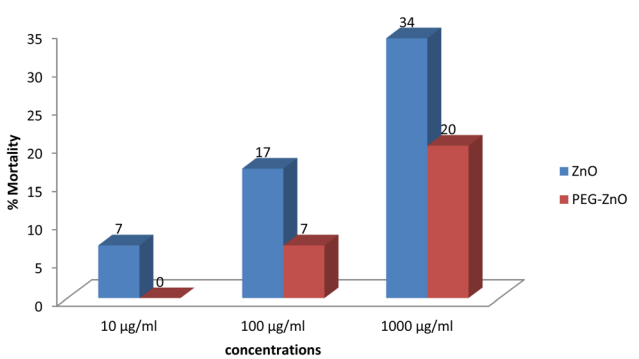

Fig. 9 Brine shrimps cytotoxic activities of the plain and PEG-ZnO.

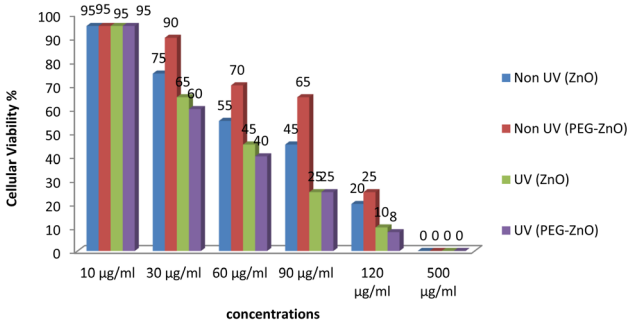

Fig. 10 Photodynamic antibacterial activities of the plain and PEG-ZnO.

cells indicated heightened toxicity, even at lower dosages of 30 and 40 µg ml^{-1}, as depicted in the figure. Conversely, PEGylated ZnO NPs displayed a mostly non-toxic profile across various concentrations. Nevertheless, concentrations exceeding 150 µg ml^{-1} exhibited a reduction in cellular viability. Interestingly, UV-exposed cells exhibited somewhat similar outcomes to those exposed to unmodified ZnO NPs.This shows the efficacy of ZnO NPs as effective photosensitizers (PS) to be use in photodynamic therapy (PDT). When exposed to light these semiconductors releases their valence electrons and aids in production of reactive oxygen species which are responsible for initiating the apoptotic cellular pathway (Fig. 10).

Discussion

Our main focus of our research was the controlled size synthesis of plain and PEGylated ZnO nanoparticles (NPs), for its biological applications,[14] therefore, it was important to evaluate the effectiveness of both the plain and PEGylated ZnO nanoparticles (NPs) against six distinct strains of multi-drug resistant (MDR) bacteria. The results we obtained yielded very promising outcomes. Literature shows that ZnO nanoparticles with different actions against *E. coli* are also involved in the signal transduction, material transport, energy metabolism and other biological processes.[14,15] Plain ZnO NPs exhibited antibacterial activity against all bacterial strains, while the PEGylated ZnO NPs demonstrated even greater efficacy compared to their non-PEGylated counterparts. It is evident that any modification like Ag-dop-ZnO NP has shown higher antibacterial activity against *Streptococcus* as compared to Plain NPs.[16] This heightened antibacterial activity observed in our synthesized ZnO NPs can be attributed to their small particle size and their ability to generate reactive oxygen species (ROS) within bacterial cells, reduction in the particle size has a significant relationship with the generation of ROS within prokaryotic cells.[17] Reports of increase Zn^{2+} concentrations inside the living cell have also been published,[18] resulting in the apoptosis of the bacterial cell. Increase in the retention time of our NPs inside bacterial cell due to PEG coating also aids in the bacterial cell lysis and hence more antibacterial efficacy. An interesting finding was that the reactive oxygen species ROS generated by the nanoparticles (NPs) exhibited bactericidal effects, but were relatively less toxic to human blood cells. K. H. Tam and colleagues have previously reported on the antibacterial activity of ZnO nanorods against *E. coli* and *B. atrophaeus*, observing that damage to the cell membrane was the cause of the antibacterial activity of ZnO against both organisms.[19] The chemiluminescence (CL) assay was employed to detect the production of hydrogen peroxide from ZnO nanorods, which induced perforations in the bacterial cell wall and resulted in the death of the bacteria.[19] The impact of ZnO nanoparticles (NPs) on *A. baumannii*, a multi-drug resistant pathogen, was investigated by Vishvanath Tiwari and colleagues. ZnO NPs were found to be effective against this pathogenic bacterium, and their mechanism of action involved leakage of reducing sugars, proteins, and DNA from the bacterial membrane. The production of ROS was identified as the cause of this membrane leakage.[20]

In a study conducted by Dhaneswar Das and colleagues, the hemolytic potential of ZnO NPs was assessed at varying concentrations. Their findings indicated that ZnO NPs exhibited minimal hemolytic activity, with only 2.5% hemolysis observed at a concentration of 2.5 mg ml^{-1}. Hemolysis is considered a reliable method for assessing the nanoparticles biocompatibility. Our samples proved to be non-toxic at most of the concentrations, particularly PEG-coated which showed only 1.5% hemolysis (70 µg ml^{-1}). Since 5% is a permissible limit therefore we can say that our samples were biocompatible.[10] Our results have similarity with the literature, highlighted the minimal hemolytic activity of ZnO NPs. Our PEG-coated samples, specifically, exhibited an even lower hemolysis rate at 1.5% (70 µg ml^{-1}), underscoring the robust biocompatibility of our synthesized nanoparticles within the permissible limit of 5%.

Krishnasamy and their research team conducted an inquiry into the cytotoxic repercussions of phytogenic ZnO nanoparticles (NPs). They determined that a concentration of 51.25 µg ml^{-1} exhibited significant cytotoxicity toward A549 cells, primarily attributed to the release of zinc ions, subsequently triggering cellular apoptosis. Additionally, further investigations established that ZnO NPs induced cell cycle arrest at the G1 phase.[21] Our results are aligned with previous studies, confirming the cytotoxic impact of ZnO NPs. Jasim and their colleagues also examined into the cytotoxic impacts of ZnO nanoparticles (NPs) on colon cancer cell lines. Their study disclosed that, owing to their diminutive size and unique surface properties, ZnO NPs could readily infiltrate tumor cells.[22] The MTT assay demonstrated that double dilution concentrations of 15 µg ml^{-1} and 8 µg ml^{-1} were highly toxic and exhibited the most potent antitumor activity against the cancer cell line, resulting in reduced tumor growth. These findings suggest that ZnO NPs may have potential as antitumor drugs for cancer treatment.[22,23] We observed almost the same efficacy, thus, our results underscore the significant cytotoxic effects at similar concentrations, indicating the potential of ZnO NPs as promising candidates for antitumor drug development. ZnO has been used in a multiple biological application, conjugation with folic acid and its application against glioblastoma cells has demonstrated significant cytotoxic effects during both the time

and dose-dependent manner.[24] Thus ZnO is recommended is one of the best candidate for nono-medicine.

Conclusion

The current work focused on synthesizing small ZnO nanoparticles (NPs) *via* a tailored wet chemical process and creating core–shell structures using polyethylene glycol (PEG) as the shell component. Advanced techniques confirmed the synthesis, size, and shape of these NPs, which were clustered and averaged 5.343 nm in size. These NPs, both in plain and core–shell forms, were tested for their antibacterial properties against multi-drug resistant bacteria strains, showing impressive results at concentrations of 500, 1000, and 1500 μg ml^{-1}. Core–shell NPs displayed superior antibacterial effectiveness and demonstrated biocompatibility with human red blood cells due to the presence of PEG. The study also explored these NPs as photosensitizers for cancer treatment through photodynamic therapy (PDT). The NPs generated reactive oxygen species (ROS) in tumor cells upon irradiation, leading to apoptosis and cell death, making them potential candidates for PDT in cancer therapy. In addition, the research investigated the cytotoxic effects of these NPs on various cell lines, including A549, colon cancer cells, and glioblastoma cells, demonstrating cytotoxic potential and potential applications in antitumor therapy. Overall, this research highlights the promising applications of ZnO NPs in antibacterial activities and cancer therapy, emphasizing their biocompatibility and safety for various biological systems. This opens the door to innovative applications in biomedical fields, improving human health and quality of life.

In conclusion, our comprehensive study sheds light on the multifaceted applications of ZnO nanoparticles, ranging from antibacterial efficacy to biocompatibility and potential antitumor activity. The mechanism of action, supported by comparative studies and explorations into cytotoxicity, enhances our understanding of the therapeutic potential of ZnO NPs. Further investigations into targeted therapeutics hold promise for advancing the clinical applications of our synthesized nanoparticles.

Conflicts of interest

There are no conflicts to declare.

Acknowledgements

The authors extend their appreciation to the Deanship of Scientific Research at King Khalid University (Abha, Saudi Arabia) for funding this work through Research Groups Program under grant number (RGP.2/71/44).

References

1 S. Chakraborty and P. Kumbhakar, Observation of exciton–phonon coupling and enhanced photoluminescence emission in ZnO nanotwins synthesized by a simple wet chemical approach, *Mater. Lett.*, 2013, **100**, 40–43.
2 P. C. Patel, S. Ghosh and P. Srivastava, Structural, magnetic and optical properties of ZnO nanostructures converted from ZnS nanoparticles, *Mater. Res. Bull.*, 2016, **81**, 85–92.
3 F. S. Jebel and H. Almasi, Morphological, physical, antimicrobial and release properties of ZnO nanoparticles-loaded bacterial cellulose films, *Carbohydr. Polym.*, 2016, **149**, 8–19.
4 S. Fatahian, *et al.*, Biodistribution and toxicity assessment of radiolabeled and DMSA coated ferrite nanoparticles in mice, *J. Radioanal. Nucl. Chem.*, 2012, **293**(3), 915–921.
5 P. Hajshafii, S. Fatahian and K. Shahanipoor, In vivo toxicity assessment of bovine serum albumin and dimercaptosuccinic acid coated Fe3O4 nanoparticles, *Iran. J. Biotechnol.*, 2014, **12**(2), 63–68.
6 X. Cheng, *et al.*, ZnO nanoparticulate thin film: preparation, characterization and gas-sensing property, *Sens. Actuators, B*, 2004, **102**(2), 248–252.
7 G. Nabiyouni, A. Barati and M. Saadat, Surface adsorption of polyethylene glycol and polyvinyl alcohol with variable molecular weights on zinc oxide nanoparticles, *Iran. J. Chem. Eng.*, 2011, **8**, 20–30.
8 R. Manjunatha, K. Usharani and D. Naik, Synthesis and characterization of ZnO nanoparticles: a review, *J. Pharmacogn. Phytochem.*, 2019, **8**(3), 1095–1101.
9 J. Alimunnisa, K. Ravichandran and K. Meena, Synthesis and characterization of Ag@ SiO2 core-shell nanoparticles for antibacterial and environmental applications, *J. Mol. Liq.*, 2017, **231**, 281–287.
10 D. Das, *et al.*, Synthesis of ZnO nanoparticles and evaluation of antioxidant and cytotoxic activity, *Colloids Surf., B*, 2013, **111**, 556–560.
11 A. Nadhman, *et al.*, Visible-light-responsive ZnCuO nanoparticles: benign photodynamic killers of infectious protozoans, *Int. J. Nanomed.*, 2015, **10**, 6891.
12 W. Muhammad, Why Brine shrimp (*Artemia salina*) larvae is used as system for nanomaterials? The science of procedure and nano-toxicology: a review, *Int. J. Biosci.*, 2019, **14**(5), 156–176.
13 K. Hayat, *et al.*, The potential of PEGylated BaMnO3 nanoparticles as drug delivery agents, *Laser Phys. Lett.*, 2013, **10**(2), 025603.
14 X. Zhu, *et al.*, Dissection of the antibacterial mechanism of zinc oxide nanoparticles with manipulable nanoscale morphologies, *J. Hazard. Mater.*, 2022, **430**, 128436.
15 S. Sheikhi, M. Aliannezhadi and F. S. Tehrani, The effect of PEGylation on optical and structural properties of ZnO nanostructures for photocatalyst and photodynamic applications, *Mater. Today Commun.*, 2023, **34**, 105103.
16 A. Forutan Mirhosseini, *et al.*, Ag-ZnO nanoparticles: synthesis, characterization, antibacterial activity on *S. mutans*, along with cytotoxic effect on U87 cell line, *Nanomed. Res. J.*, 2022, **7**(3), 254–263.
17 A. Khalid, *et al.*, Cytotoxicity of zinc oxide nanoparticles coupled with folic acid and polyethylene glycol, *Dig. J. Nanomater. Biostruct.*, 2022, **17**(1), 73.

18 F. Mohammad, *et al.*, Influence of surface coating towards the controlled toxicity of ZnO nanoparticles in vitro, *Coatings*, 2023, **13**(1), 172.
19 K. Tam, *et al.*, Antibacterial activity of ZnO nanorods prepared by a hydrothermal method, *Thin Solid Films*, 2008, **516**(18), 6167–6174.
20 V. Tiwari, *et al.*, Mechanism of anti-bacterial activity of zinc oxide nanoparticle against carbapenem-resistant *Acinetobacter baumannii*, *Front. Microbiol.*, 2018, **9**, 1218.
21 K. S. Rajkumar, *et al.*, Facile biofabrication, characterization, evaluation of photocatalytic, antipathogenic activity and in vitro cytotoxicity of zinc oxide nanoparticles, *Biocatal. Agric. Biotechnol.*, 2019, **22**, 101436.
22 S. A. Jasim and N. A. Saleh, The Cytotoxic Effect of Zinc Oxide on Colon Cancer Cell Lines in Vitro, *Indian J. Public Health Res. Dev.*, 2019, **10**(10), 2638.
23 E. Grela, J. Kozłowska and A. Grabowiecka, Current methodology of MTT assay in bacteria–a review, *Acta Histochem.*, 2018, **120**(4), 303–311.
24 Z. H. Marfavi, *et al.*, Glioblastoma U-87MG tumour cells suppressed by ZnO folic acid-conjugated nanoparticles: an in vitro study, *Artif. Cells, Nanomed., Biotechnol.*, 2019, **47**(1), 2783–2790.